

## **A PRACTICAL REAL-TIME POWER QUALITY EVENT MONITORING APPLICATIONS USING DISCRETE WAVELET TRANSFORM AND ARTIFICIAL NEURAL NETWORK**

M. ISMAIL GURSOY<sup>1,\*</sup>, A. SERDAR YILMAZ<sup>2</sup>, S. VAKKAS USTUN<sup>3</sup>

<sup>1</sup>Dept. of Electric and Energy, Vocational School of Technical Science,  
Adıyaman University, Adıyaman, Turkey

<sup>2</sup>Department of Electrical and Electronics Engineering,  
Kahramanmaraş Sütçü İmam University, Kahramanmaraş, Turkey

<sup>3</sup>Department of Electrical and Electronics Engineering,  
Adıyaman University, Adıyaman, Turkey

\*Corresponding Author: mgursoy@adiyaman.edu.tr

### **Abstract**

Determining the events that affect Power Quality (PQ) disturbances is remarkable for consumers. The most important aspects in the assessment of PQ disturbances are real-time monitoring of PQ disturbances and their fast interpretation. In this study, Artificial Neural Networks (ANNs) was used as a classifier benefiting from estimated parameters in PQ disturbances based on Discrete Wavelet Transform (DWT) on the real-time environment for determining the disturbances in power systems. Voltage signals (sag, swell, interruption, transient, harmonic and normal) used in this study were recorded from real grids. DWT was used for featuring the extraction and calculation of the wavelet coefficients, and subsequently, calculated energy levels were used as an input to ANN. The results revealed analyzing the real data processed with DWT and ANN with 100% accuracy proved the superiority of this study. Based on the results of this study, identification of real-time PQ disturbances provided an important advantage for the firms and industry. Particularly, the reasons for the failures in the system related to PQ disturbances were simultaneously diagnosed, as well.

Keywords: Artificial neural networks, Detection of power quality, Discrete wavelet transform, Real-time monitoring.

### **1. Introduction**

Although both new appliances produced as a result of developed technology and the ones used previously have increased life quality of the consumers, these

**Nomenclatures**

$a_j$	Scaling coefficient
$d_j$	Wavelet coefficient
$f(n)$	Discrete signal
$f(t)$	Input signal
$g(n)$	High pass filter
$h(n)$	Low pass filter

**Greek Symbols**

$\Phi$	Scaling function
$\Psi$	Wavelet function

**Abbreviations**

ANN	Artificial Neural Network
CWT	Continuous Wavelet Transform
DWT	Discrete Wavelet Transform
EMD	Empirical Mode Decomposition
FT	Fourier Transform
GT	Gabor Transform
HHT	Hilbert Huang Transform
HT	Hilbert Transform
IMF	Intrinsic Mode Function
PQ	Power Quality
ST	S-Transform
STFT	Short Time Fourier Transform

appliances have seriously led to the electrical breakdown of the networks they feed from the pure sinusoidal wave pattern. Thus, the operation of factories in the industry is negatively affected by this. In addition, this causes many problems like damaging of equipment in power systems, electronic power circuits of microcontrollers and high-technology tools [1]. PQ disturbance also leads to several problems like a failure in loads, instability and short lifetime [2].

Power Systems have been designed in a way taking sinusoidal voltage with certain frequency and amplitude as a reference. Incidents occurring in PQ appear as any disturbances on the amplitude, frequency or wave type of the voltage. Parameters defining the electrical PQ are arranged as short-term voltage sags/swells, over-voltages and under-voltages, harmonics, instabilities between phases and voltage fluctuations according to IEC 61000-4-30 standard [3]. In power systems, PQ is an important factor. PQ can be defined as supplying a noiseless and steady power for the consumers [4].

In the literature, different methods have been used to form a feature extract so as to locate the disturbances in the power system. These methods are frequently based on the purpose of determining the time-frequency dispersion with methods like Fourier Transform (FT), Short-Term Fourier Transform (STFT), S-Transform (ST), Wavelet Transform (WT), Hilbert Huang Transform (HHT) and Gabor Transform (GT). In addition, they also depend on revealing determinant features representing the original sign through energy, entropy and various statistical processes and decreasing the data size.

FT is usually used in specifying the harmonic components in the signal. PQ disturbances are unstable signals. A window function is used in methods employing STFT; however, STFT requires a great number of calculations [5]. S-Transform is a time-frequency analysis method like STFT and WT. In this method, the analysis is performed in frequency domain changing the position in Gaussian function as a special window function [6]. WT method and feature extraction tools are applied for determining the PQ disturbances, [7]. WT is used in unstable signals and reveals good results, but the performance of management decreases in noisy signals. HHT has a wide area of usage in the analysis of nonlinear and non-stationary signals. It consists of two main parts:

Empirical Mode Decomposition (EMD) and Hilbert Transform (HT) [8]. EMD is separated into different frequency components called Intrinsic Mode Function (IMF). Being separated into components by EMD, these signals can be analyzed for their frequency, amplitude and phases amplitude via HT [9]. GT is a developed function of STFT. GT is defined as time-frequency analysis taking FT of a window function to be selected in the time domain. GT is a special form of the STFT that uses the Gaussian Window Function [10].

ANN Systems are used as an effective method for classifying the problems of PQ disturbances. ANN Systems are used in classification architecture based on complex feature parameters like frequency components and wave types [11-13].

Most of the devices measuring PQ disturbances calculates RMS values of current and voltage, power factor, power values, and harmonic components. Classification of PQ disturbances is hard in terms of time and costs due to complex algorithms. Classification of PQ disturbances is calculated with a PC recording required parameters instead of embedded systems [14]. In this study, Haar function was used for obtaining the feature vector. Because Haar function makes calculations in less time with less load of the process, the processes could be conducted at the real-time. Because the Db4 function is generally used in PQ disturbances and this function has more load of the process, it has not been used in real-time analyses [13].

In this study, it was aimed to develop an intelligent event recognition and classification technique that was effective, reliable and had a robust structure for determining the PQ disturbances. With this study, a new PQ monitoring system, a hardware structure of this system and a software architecture were designed. Power system operators and consumers connected to the power systems were aimed to monitor the PQ parameters of the system with the help of designed PQ monitoring system easily. It was also aimed to provide advantages such as taking necessary precautions detecting the factors causing disruption in PQ.

The PQ monitoring device designed for the study was placed in both the welding workshop of Vocational School of Technical Sciences and Machine department, Electrical and Energy department electrical machines laboratory, which were located in Adiyaman University campus and in the concrete plant located in the centre of Adiyaman/Turkey.

## 2. Essentials of Wavelet Transform

WT is a time-frequency transform method, which has recently been used for analyzing PQ disturbances. Wavelet Decomposition technique is a powerful tool employed in the assessment of PQ disturbances [12] and is used for the analysis of

stable and unstable signals [15]. The greatest feature of WT distinguishing it from FT is that while only frequency information is acquired in FT, the acquired data consist of both frequency and time information in WT [16]. So that the times when all frequency changes appear in analysis of the system can sensitively be determined. One of the important properties of WT it is having a wide window width for low-frequencies while also having a narrow width for high-frequencies. Thus, it is possible to provide optimum time-frequency resolution at all frequency ranges [17].

WT is examined in two ways, Continuous Wavelet Transform (CWT) and DWT. Since CWT uses all scales in calculations and gives many details about the signal calculation of coefficients of wavelets, it is difficult and time-consuming. In DWT, wavelet coefficients are calculated only for discrete time scales rather than all-time scales. Thus, analysis can be more easily performed in a shorter period. Therefore, DWT is used more frequently [18].

For a given  $f(t)$  signal,  $K$  level of DWT, with both wavelet function and scaling function, can be defined as Eq. (1) [13].

$$f(t) = \sum_n a_j(n) \phi(t-n) + \sum_n \sum_{j=0}^{J-1} d_j(n) 2^{j/2} \psi(2^j t-n) \tag{1}$$

where  $a_j$  is the  $J$ th scaling coefficient,  $d_j$  is  $j$ th wavelet coefficient,  $\phi(t)$  is scaling function,  $\Psi(t)$  is wavelet function,  $J$  represents the highest level of wavelet transform and  $t$  represents time. Scaling function and wavelet function are used to separate the sign in different resolution levels in multi-resolution decomposition. Wavelet function detail coefficients are  $a_j$  Eq. (2) and scaling function approach coefficients are  $d_j$  Eq. (3) for the separated signal with Wavelet transform.

$$a_{j+1}(n) = \sum_k h(m-2n) a_j(n) \tag{2}$$

$$d_{j+1}(n) = \sum_m g(m-2n) a_j(n) \tag{3}$$

where;  $h$  denotes coefficients of the low pass filter and  $g$  denotes the coefficients of the high pass filter [19].

**2.1. Parseval’s Theorem in DWT**

According to Parseval’s Theorem, for a discrete  $f(n)$  signal, the energy dissipated on the resistance in the frequency region equals to the sum of the squares of the spectrum coefficients of Fourier transform.

$$\frac{1}{N} \sum_n |f(n)|^2 = \sum_k |c_k|^2 \tag{4}$$

where;  $N$  is the number of samples and  $c_k$  denotes the spectrum coefficients of Fourier transform. To apply Parseval’s Theorem to DWT method, we can obtain the following equation regarding Eqs. (1) and (4).

$$\frac{1}{N} \sum_t |f(t)|^2 = \frac{1}{N_j} \sum_k |a_j(k)|^2 + \sum_{j=1}^J \left( \frac{1}{N} \sum_k |d_j(k)|^2 \right) \tag{5}$$

Therefore, the energy of the disturbed signal can be obtained by Eq. (5). In this equation, the first term on the right represents the approximate level of the discrete

signal, while the second term states the detail level of the discrete signal [20]. This second term representing the detail levels of the disturbed signal is used in feature extraction process of the PQ disturbances.

### 3. Artificial Neural Networks

ANNs are information processing units developed regarding the biologic neural system. The most important feature of it is that it can learn from experiences. ANNs have been developed for automatically fulfilling the abilities of human brain like creating and forming new information and discovering through learning. A neural network includes connected cells in layers and networks connecting these layers (Fig. 1).

In classifications of PQ disturbances, as a final stage, they were classified with the method of neural network management. And the input neuron number, hidden layer number, neuron number and output neuron number were found to be 9, 1, 11, and 6, respectively.

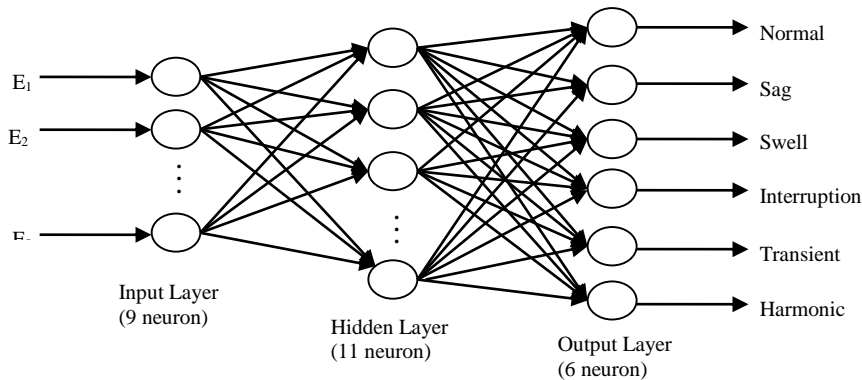


Fig. 1. Typical architecture of ANN.

### 4. Data Set (Experimental Setup)

In this study, the data used in PQ disturbances' classification were recorded as being directly measured by different companies at different times.

It was aimed to classify PQ disturbances in real-time. A PQ monitoring device (Fig. 2) was designed using a dsPIC33FJ128GP804 microcontroller. The microcontroller with 40 MIBS processor speed had 128 kB program memory. The program codes developed by MPLAB interface were prepared by C compiler.

The grid voltage signals were recorded with 6.4 kHz sampling frequency from measurement points determined with PQ monitoring device. Totally, 1280 data including 128 data in each period out of 10 periods were saved for the analysis.

The wavelet coefficients of this data were found with WT method using MATLAB program. The feature vector was obtained calculating the energy levels of the wavelet coefficients with the help of Parseval theorem. The model was created by training process with ANN classification method. The obtained model coefficients were uploaded on the microcontroller.

The feature vector of the voltage signals recorded on the variable was calculated using WT and Parseval theorem. The obtained feature vectors were classified with

ANN training coefficients. Classified PQ disturbances were recorded on SD card in the monitoring device. When there was no PQ disturbance, the normal grid voltage signal analysis was performed, and "normal" recording was conducted on the memory card.

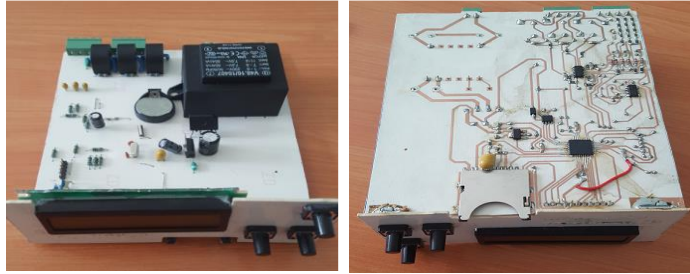


**Fig. 2. Grid voltage monitoring device.**

The PQ monitoring device designed as microcontroller-based was connected to the measuring points specified in the power grid in a single phase. The phase voltage values to which they were connected were recorded with a sampling frequency of 6.4 kHz. Two different variables were defined in the software architecture. While the voltage values were recorded in one of the variables, the other saved data were analyzed with statistical operations. As shown in Fig. 3, while a period of 200 ms was recorded for a period of 10 ms, analysis of data recorded in the variable *b* for the previous 200 ms period was performed in these analyzes; the feature vector was calculated in 93.47 ms. At 3.34 ms, the feature vector was classified as PQ disturbances according to the ANN method. Disturbance types classified for 6,63 ms were saved in the memory card in the PQ monitoring device. The data of *a* variable for 96.56 ms. waited to be saved. Statistical analyzes were performed when *a* variable was recorded at the end of 200 ms. While analysis was made in *a* variable, the data was again saved in variable *b*. This process continued in a continuous infinite loop.

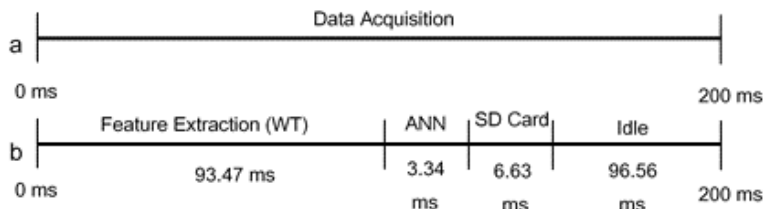


**Fig. 3. Real-time monitoring duty cycle.**

#### 4.1. Feature extraction

Each coefficient of WT could be separated in their own energy levels and in their frequency period. Ranges of frequency bands in high-resolution Wavelet Transform Decomposition were presented in Table 1. WT coefficients could be used to associate the energies obtained using Parseval's Theorem with every PQ disturbances in voltage signals.

In this study, Haar function was chosen as the wavelet function. Wavelet Haar made us have less workload and faster analyses possible. Coefficients for nine levels were acquired using DWT with Haar function. Energy levels were obtained through DWT Coefficients and Parseval’s Theorem.

**Table 1. Ranges of frequency bands in high-resolution decomposition.**

Decomposition Levels	Frequency Range(Hz)
d1	3200-1600
d2	1600-800
d3	800-400
d4	400-200
d5	200-100
d6	100-50
d7	50-25
d8	25-12,5
d9	12,5-6,25
a9	12,5-6,25

**4.2. Classification**

In the ANN classification method, nine energy levels calculated with Parseval Theorem using DWT coefficients were taken as input. A hidden layer with 11 neurons was used. Output layer had six neurons because of six different PQ because of six different PQ disturbances neurons were used. Output layer had six neurons because of six different PQ disturbances. A developed classification algorithm was presented in Fig. 4.

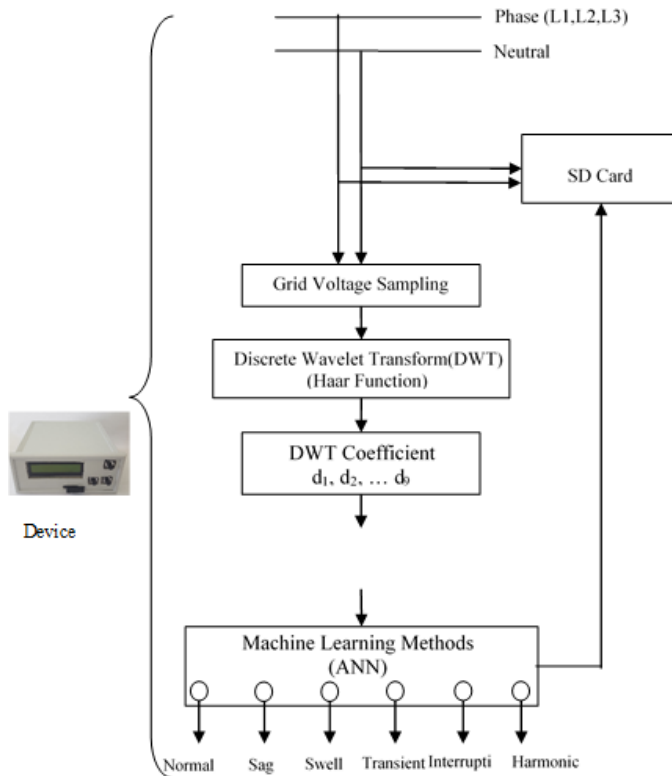


**Fig. 4. Proposed method for the classification of PQ disturbances.**

## **5. Results**

In this study, PQ disturbances were classified with nine energy distribution patterns in the wavelet domain. In the obtained data, while x-axis indicated time, y-axis was voltage amplitude over per unit. The samples were recorded for 10 periods of 200 milliseconds with developed grid monitoring device, and their graph was drawn with MATLAB software. Every disturbance sign recorded through electronic application circuit was primarily separated into nine levels with Haar Wavelet filter, and subsequently, its detail energy levels were acquired with the Parseval's Theorem (Eq. 5). In literature, db4 wavelet filter of the DWT was noticed to be used frequently. In this study, these processes were completed with less workload in a shorter time using Haar filters.

### **5.1. Normal**

In Figs. 5 (a) and (b), normal signal and energy decomposition of this normal signal when no PQ disturbances occurred were shown. Normal signals were classified as a reference to other PQ disturbances.

In Figs.5(c) and (d), E7 corresponded to 50 Hz value which was the fundamental frequency component of the energy-level power grids. E3, E4 and E5 energy levels indicated harmonic components in normal signals as the odd harmonic values were more visible in the power grids. E1 and E2 indicated high-frequency components of energy levels. No significant changes occurred in E1 and E2 energy levels in cases where there were no high-frequency PQ disturbances in power grids. Since E8 and E9 energy levels corresponded to components with smaller values than the fundamental frequency value, there was no change in these levels. The energy distributions of the analyzed signals corresponded to DWT frequency bands as shown in Table 1.

### **5.2. Swell**

Swell occurred when there was a 10% increase in the amplitude of the voltage signals in Fig. 7(a) and (b).

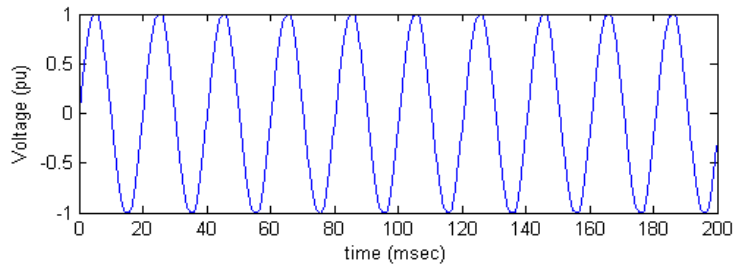
It was seen that as a result of the disturbance, a rise in the energy levels of the DWT coefficients appears Figs. 6(c) and (d). As result of voltage swell that was noticed in Figs. 6(c) and (d), especially E7 component with 50 Hz. basic frequency band, the normal sine signal had a larger value than the energy level E7. Since there was no frequency difference in the voltage of the grid after the swell, the amplitudes of the energy levels increased proportionally. In case of voltage swell events, there was no change in the values of E8 and E9 energy levels as there were not any lower frequencies than the fundamental frequency.

### **5.3. Transient**

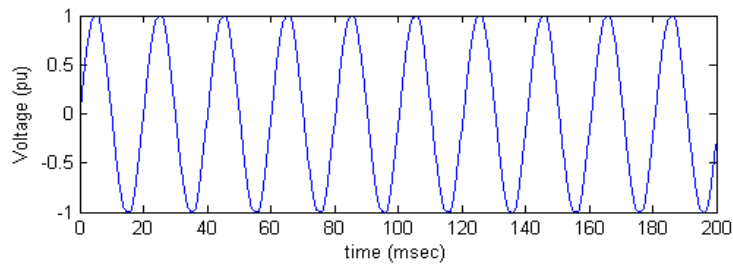
Temporary disturbances like beats lasted from 50 nanoseconds to one millisecond, and they could reach up to sudden high voltage values. Temporary events mainly occurred due to capacitor switching and harmonic distortion Figs. 8(a) and (b).

Transient events showed a large change (increase) in energy levels E2, E3, E4 and E5 as there were high-frequency components in PQ disturbances. E7 energy level corresponded to the fundamental frequency value of 50 Hz. In transient events

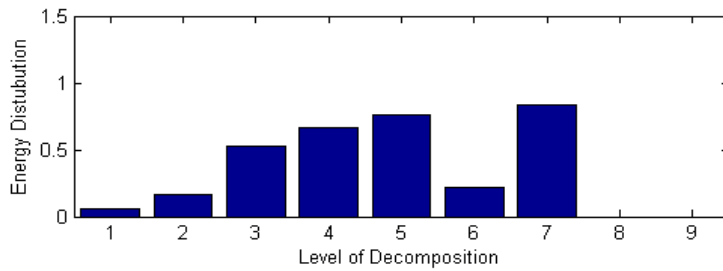
of PQ disturbances, values of E8 and E9 energy levels were observed as low since low-frequency components were not usually found in Figs. 8(c) and (d).



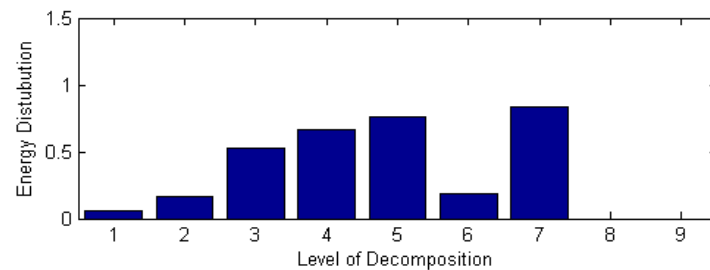
(a) Normal-1 signal waveform.



(b) Normal-2 signal waveform.

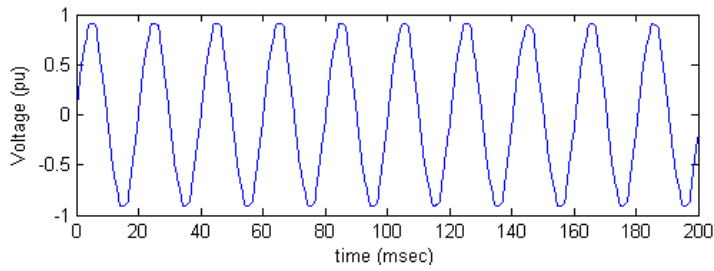


(c) Energy distribution for nine decomposition levels of the normal-1 signal.

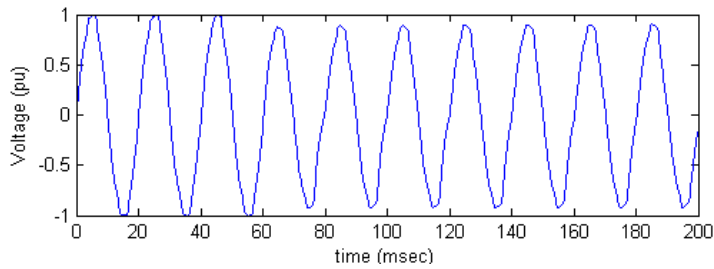


(d) Energy distribution for nine decomposition levels of the normal-2 signal.

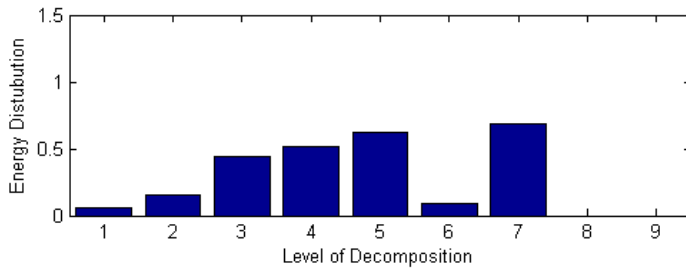
Fig. 5. Normal signal.



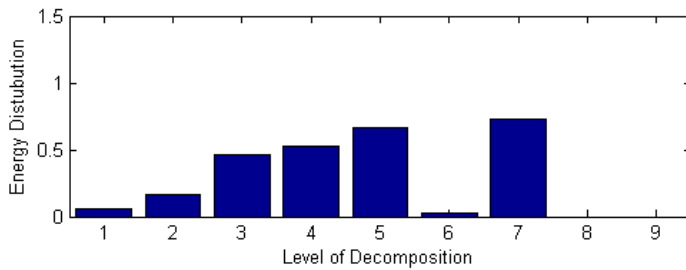
(a) Sag-1 signal waveform.



(b) Sag-2 signal waveform.

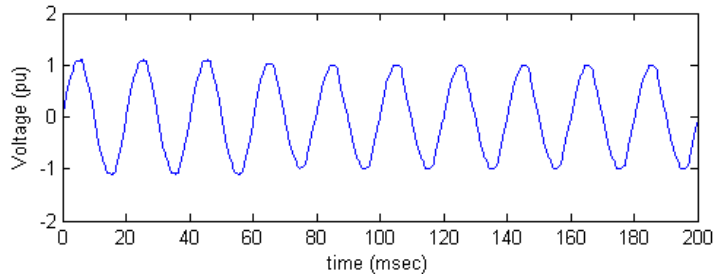


(c) Energy distribution for nine decomposition levels of the sag-1 signal.

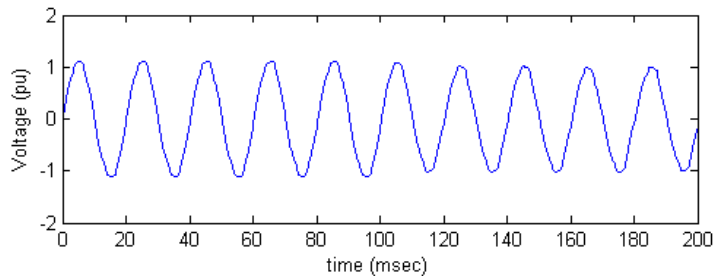


(d) Energy distribution for nine decomposition levels of the sag-2 signal.

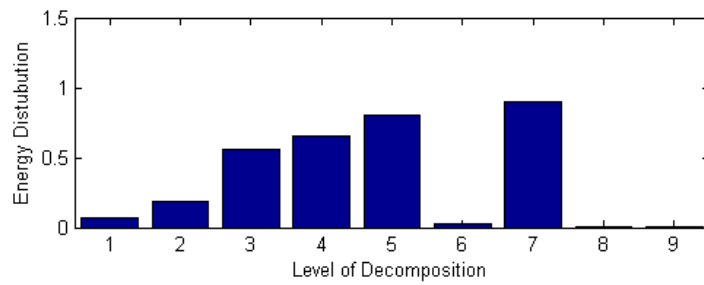
Fig. 6. Sag signal.



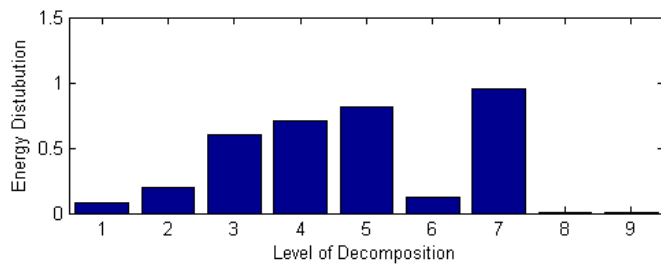
(a) Swell-1 signal waveform.



(b) Swell-2 signal waveform.

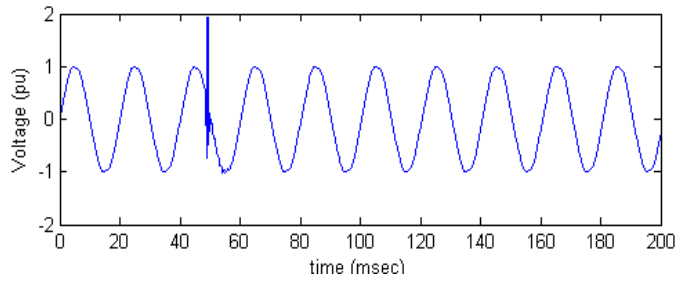


(c) Energy distribution for nine decomposition levels of the swell-1 signal.

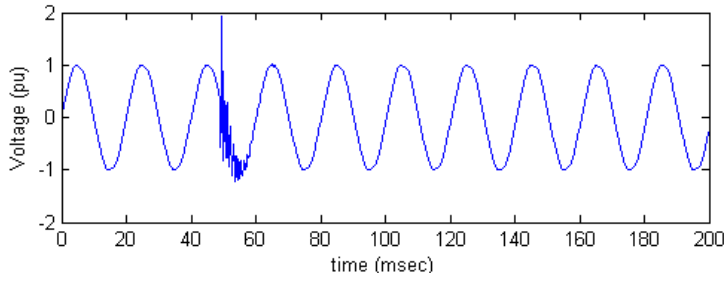


(d) Energy distribution for nine decomposition levels of the swell-2 signal.

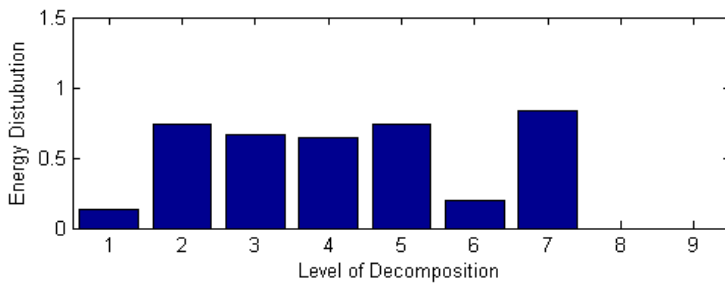
Fig. 7. Swell signal.



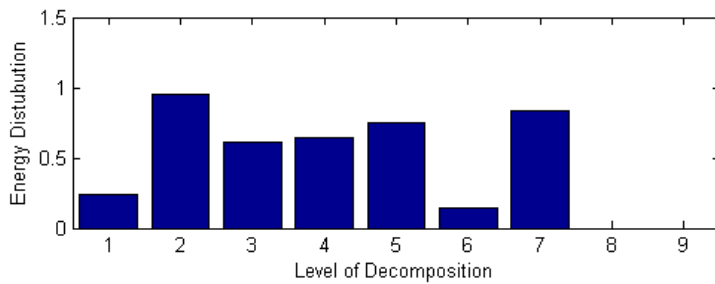
**(a) Transient-1 signal waveform.**



**(b) Transient-2 signal waveform.**



**(c) Energy distribution for nine decomposition levels of the transient-1 signal.**



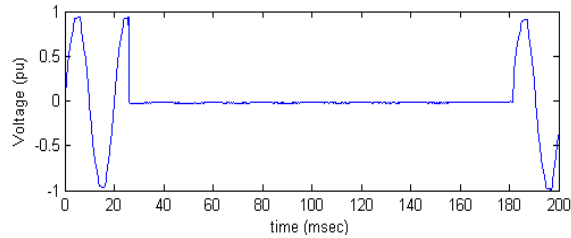
**(d) Energy distribution for nine decomposition levels of the transient-2 signal.**

**Fig. 8. Transient signal.**

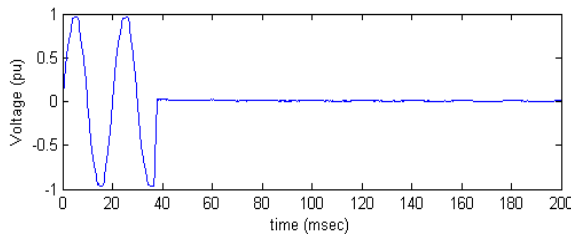
### 5.4. Interruption

The interruption could appear when a power system had failures as result of malfunctioning of control systems. This interruption could last from 0,5 period to 1 minute in Figs. 9(a) and (b).

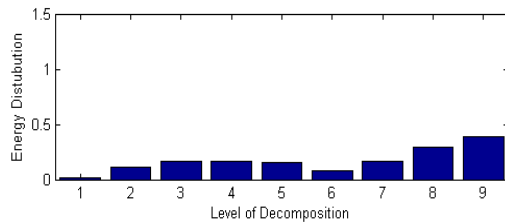
As could be seen in Figs. 9(c) and (d) the energy levels had decreased at the end of voltage's falling to values of zero or close to zero as result of interruption. The values in the energy levels dropped to the level of 0.25 pu. As result of interruption, the normal signal energy level was 0.95 pu.



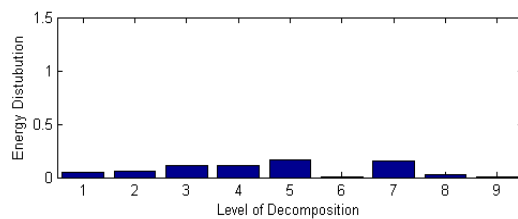
(a) Interruption-1 signal waveform.



(b) Interruption-2 signal waveform.



(c) Energy distribution for nine decomposition levels of the interruption-1 signal.

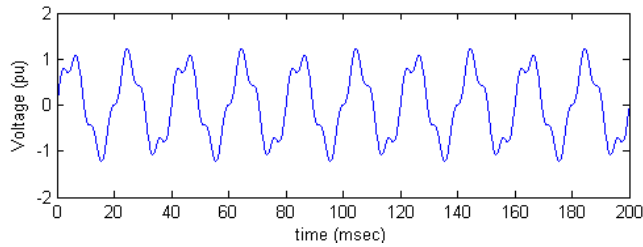


(d) Energy distribution for nine decomposition levels of the interruption-2 signal.

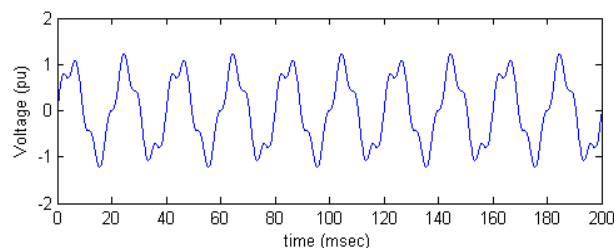
Fig. 9. Interruption signal.

### 5.5. Harmonic

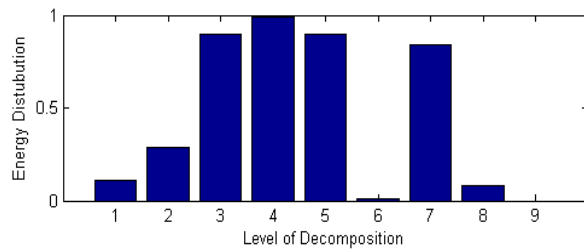
Harmonics was a destructive effect taking place as a frequent compound of sinusoidal voltage and had a sinusoidal form. Semi-conductor components could be ranked as one of the most important reasons. Since harmonic PQ disturbances rarely happened on grid voltages, data belonging to these PQ disturbances were produced by MATLAB Figs. 10(a) and (b). Analyses were conducted producing harmonic signals with THD values changing between 8 and 15.



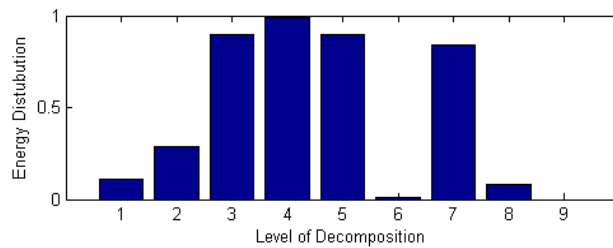
(a) Harmonic-1 signal waveform.



(b) Harmonic-2 signal waveform.



(c) Energy distribution for nine decomposition levels of the harmonic-1 signal.



(d) Energy distribution for nine decomposition levels of the harmonic-2 signal.

Fig. 10. Harmonic signal.

Acquired energy distributions were classified utilizing from ANN method. The ANN system was developed using C codes. The parameters used in ANN were:

- Input Layer Neuron : 9
- Hidden Layer : 1
- Hidden Layer Neuron : 11
- Output Layer Neuron : 6
- Training Sample Number : 90 (15 samples for every disturbance)
- Activation Function : Sigmoid Function

A rule of thumb was used to select a number of the neurons and layers of the ANN. The error rate during the training process was 0.001. Each PQ disturbance was analyzed with nine levels of DWT. Six different PQ disturbances frequencies of the acquired results and their amplitudes were examined according to IEEE standards [3].

Acquired DWT coefficients were classified with ANNs method. The results obtained with classification method were presented in Table 2. Totally, 90 datasets were used for training, and 30 datasets were used for testing. The confusion matrix representing PQ disturbances identified in ANN classification was shown in Fig. 11.

**Table 2. Accuracy of the classification system for each class of disturbance.**

Disturbance	Train			Test		
	Correctly Classified	Total	Accuracy (%)	Correctly Classified	Total	Accuracy (%)
Normal	15	15	100	5	5	100
Sag	15	15	100	5	5	100
Swell	15	15	100	5	5	100
Transient	15	15	100	5	5	100
Interruption	15	15	100	5	5	100
Harmonic	15	15	100	5	5	100

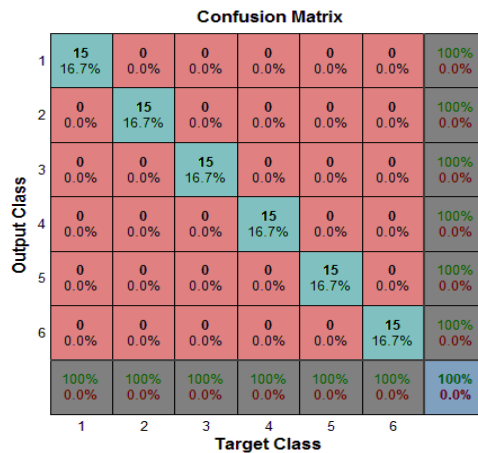


**Fig. 11. Confusion matrix of PQ disturbances.**

## 5.6. Performance Comparisons

In this section, the classification results obtained with real data were compared with the results of ANN classifiers that were evaluated as reference using the proposed algorithm. The correct classification was chosen as the criterion in the performance comparison. The comparison results were presented in Table 3.

As seen in Table 3, the classification of PQ disturbances by the proposed method was superior to that of studies carried out on noiseless conditions [21-25]. This increase in the correct classification ratio when compared with other studies could be attributed to the acquisition of energy feature vector without losing the distinguishing characteristics of the signal and the generalization ability of the ANN classifier.

**Table 3. Performance comparison of classification technique results (%).**

Disturbance Type	Ref. [21] WT-FkNN	Ref. [22] WT-ANN	Ref. [23] WT-ANN	Ref. [24] WT-ANN	Ref. [25] WT-ANN	Purposed method
Normal	-	-	100	100	100	100
Sag	97,64	100	95,4	94	99,5	100
Swell	94,11	100	95	100	100	100
Transient	94,53	100	-	100	99,5	100
Interruption	100	-	94,6	100	93	100
Harmonic	100	100	100	100	100	100

## 6. Conclusion

In this paper, ANN system was developed for classifying PQ disturbances. The real data collected from grids in a real environment and in real-time, and the disturbances from the grid were classified. Six types of common PQ disturbances were considered. The collected real data were processed with DWT Haar function, and energy levels were calculated and classified with ANN. Feature extraction and training of ANN parameters were coded in dsPIC33FJ128GP804 microcontroller.

The proposed DWT-ANN system was tested with thirty unseen real data distorted voltage signals to verify its classification accuracy. It was finally noticed that DWT-ANN system correctly classified 100% of the tested signal. Thus, the DWT-ANN system could be considered as accurate for classifying PQ disturbances.

This study was different from other studies carried out until today because of using the WT-Haar function for analyzing measurement data made on real grids. The use of Haar function provided a significant advantage on WT functions in terms of the least amount of processing in the shortest time to complete the operations. At the same time, WT showed that it was a very useful method for detecting power systems because of its convenience of providing time and frequency information together and creating software. Upon determining this, it was concluded that it could instantly be used for determining the disturbances of PQ of the power grids in real time.

## Acknowledgement

This study was supported by Kahramanmaraş Sütçü İmam University Institute of Natural and Applied Sciences as project number 2015/3-65D.

## References

- 1 Dugan, R.C.; McGranaghan, M.F.; Santoso, S.; and Beaty, H.W. (2004). *Electrical power systems quality* (2<sup>th</sup> ed.). New York: McGraw Hill.
- 2 Gaing, Z.-L.; and Huang, H.-S. (2003). Wavelet-based neural network for power disturbance classification. *Proceedings of the IEEE Power Engineering Society General Meeting*. Toronto, Canada, 1621-1628.
- 3 IEEE standard (1159-1995). *IEEE Recommended Practice for Monitoring Electric Power Quality*. IEEE.
- 4 Weng, K.K.; Wan, W.Y.; Rajkumar, R.K.; and Rajkumar, R.K. (2015). Power quality analysis for PV grid connected system using PSCAD/EMTDC. *International Journal of Renewable Energy Research*, 5(1), 121-132.
- 5 Kanirajan, P.; and Suresh Kumar, V. (2015). Power quality disturbance detection and classification using wavelet and RBFNN. *Applied Soft Computing*, 35(C), 470-481.
- 6 Stockwell, R.G.; Monsinha, L.; and Lowe, R.P. (1996). Localization of the complex spectrum: The S transform. *IEEE Transactions on Power Delivery*, 44(4), 998-1001.
- 7 Roy, S.; and Nath, S. (2012). Classification of power quality disturbances using features of signals. *International Journal of Scientific and Research Publications*, 2(11), 1-9.
- 8 Zhan, W.; Xiangjun, Z.; Xiaoxi, H.; and Jingying, H. (2012). The multi-disturbance complex power quality signal HHT detection technique. *Proceedings of the IEEE PES Innovative Smart Grid Technologie.*, Tianjin, China, 1-5.
- 9 Huang, N.E.; Shen, Z.; Long, S.R.; Wu, M.C.; Shih, H.H.; Zheng, Q.; Yen, N.-C.; Tung, C.C.; and Liu, H.H. (1998). *The empirical mode decomposition and the Hilbert Spectrum for nonlinear and non-stationary time series analysis*. Great Britain: The Royal.Society Publishing.
- 10 Cho, S.-H.; Jang, G.; and Kwon, S.-H. (2010). Time frequency analysis of power quality disturbances via the Gabor-Wigner Transform. *IEEE Transactions on Power Delivery*, 25(1), 494-499.
- 11 Gaouda, A.M.; Salama, M.M.A.; Sultan, M.R.; and Chikhani, A.Y. (1999). Power Quality detection and classification using wavelet-multiresolution signal decomposition. *IEEE Transactions on Power Delivery*, 14(4), 1469-1476.
- 12 Uyar, M.; Yildirim, S.; and Gencoglu, M.T. (2008). An effective wavelet-based feature extraction method for classification of power quality disturbance signals. *Electric Power Systems Research*, 78(10), 1747-1755.
- 13 Sharma, P.; and Saxena, A. (2017). Critical investigations on performance of ANN and wavelet fault classifiers. *Cogent Engineering*, 4(1), 1286730.
- 14 Balaji, J.; and Prasanth, B.V. (2014). DSP-FPGA Based real-time power quality disturbances classifier. *International Journal of Advanced Technology and Innovative Research*, 6(9), 1058-1062.
- 15 Santoso, S.; Powers, E.J.; Grady, W.M.; and Hofman, P. (1996). Power quality assessment via wavelet transform analysis. *IEEE Transactions on Power Delivery*, 11(2), 924-930.

- 16 Uyar, M.; Yıldırım, S.; and Gençoğlu, M.T. (2011). A pattern recognition approach for classification of power quality disturbance types. *Journal of Faculty of Engineering and Architecture of Gazi University*, 26(1), 41-56.
- 17 Daubechies, I. (1990). The wavelet transform time frequency localization and signal analysis. *IEEE Transaction on Information Theory*, 36(5), 961-1005.
- 18 Yılmaz, D.; and Bayhan, S. (2009). Detection of the waveform disturbances in power systems by using wavelet transform. *Technological Applied Sciences*, 4(2), 151-162.
- 19 Sebastian, P.; and Anthony DSa, P. (2015). Implementation of a quality signal classification system using wavelet based energy distribution and neural network. *Proceedings of the International Conference on Power and Advanced Control Engineering*. Bangalore, India, 157-161.
- 20 Gaing, Z.-L. (2004). Wavelet-based neural network for power disturbance recognition and classification. *IEEE Transactions on Power Delivery*, 19(4), 1560-1568.
- 21 Panigrahi, B.K.; and Pandi, V.R. (2009). Optimal feature selection for classification of power quality disturbances using wavelet packet-based fuzzy k-nearest neighbor algorithm. *IET Generation Transmission & Distribution*. 3(3), 296-306.
- 22 Kamble, S.; and Dupare, I. (2014). Detection of power quality disturbances using wavelet transform and artificial neural network. *Proceedings of the International Conference on Magnetism, Machines & Drives (AICERA)*. Kottayam, India, 1-5.
- 23 Sebastian, P.; and Pradeep, A. (2016). A Comparative study of artificial neural network-based power quality signal classification systems with wavelet coefficients and wavelet-based energy distribution. *International Journal of Advanced Research in Electrical, Electronics and Instrumentation Engineering*. 5(4), 2929-2934.
- 24 He, Z.; Zhang, H.; Zhao, J.; and Qian, Q. (2012). Classification of power quality disturbances using quantum neural network and DS evidence fusion. *European Transactions of Electrical Power*, 22(4), 533-547.
- 25 Singh, B.; Shahani, D.T.; and Kumar, R. (2012). Recognition of power quality events using DT-DWT based complex wavelet transform. *Proceedings of the Fifth Power India Conference*. Murthal, India, 1-4.